Available online at www.sciencedirect.com
SCIENCE DIRECT®
Bioorganic & Medicinal Chemistry Letters
Bioorganic & Medicinal Chemistry Letters 14 (2004) 2877–2882

Antimelanomal activity of the copper(II) complexes of 1-substituted 5-amino-imidazole ligands against B16F10 mouse melanoma cells

Uday Sandbhor,[a,*,†] Pallavi Kulkarni,[a] Subhash Padhye,[a,*] Gopal Kundu,[b] Grahame Mackenzie[c] and Robin Pritchard[d]

[a]*Department of Chemistry, University of Pune, Pune 411007, India*
[b]*National Center for Cell Science, NCCS Complex, Pune 411007, India*
[c]*Department of Chemistry, University of Hull, Hull HU6 7RX, UK*
[d]*Department of Chemistry, UMIST, Manchester M60 1QD, UK*

Received 10 December 2003; revised 13 March 2004; accepted 15 March 2004

Abstract—The copper complexes of 5-amino-imidazole ligands were prepared and characterized by various spectroscopic techniques. The ligand geometry around the copper(II) centre is square pyramidal based on N_2O_2 donor atoms and a coordinated water molecule at the apex. Single crystal X-ray structures were determined for both ligands. Ligands and copper complexes exhibited dose-dependent antiproliferative effects on the growth of B16F10 melanoma cells line but lower IC_{50} values were observed for the copper complexes.

1. Introduction

The chemistry of imidazole compounds has been of much interest due to the presence of such heterocycles in a large variety of biologically important molecules. For example, some imidazole derivatives have shown interesting antifungal and antitumour properties.[1–3] Also, the antimicrobial activities of a series of 4-diazoimidazole-5-carboxamides bearing lipophilic substituents have been evaluated recently and compounds have been found to possess antifungal activities against both moulds as well as yeasts.[4] Furthermore, many imidazole derivatives have been used as catalysts in the synthesis of copolymers,[5,6] as ligands in anisotropic conductors[7–9] and as electron acceptors in charge-transfer solids.[10,11]

The 5-amino-imidazole nucleotides are of fundamental importance and occur in all living systems as intermediates in the de novo biosynthesis of purine nucleotides. The demand for these purine nucleotides has been shown to be elevated in tumour and virally infected cells due to high levels of de novo biosynthesis.[12] As a result, synthetic mimics or structural analogues of 5-amino-imidazoles offer a selective chemotherapeutic approach to the control of nucleic acid biosynthesis in the case of virally infected cells and tumour tissues.[13] Mackenzie et al. have described the activities of several close structural analogues of the amino-imidazole ribotide (**1**) as competitive inhibitors of the enzymes phosphoribosyl-aminoimidazole carboxylase (E.C.4.1.1.21, AIR-carboxylase) and phosphoribosyl-aminoimidazole-succinocarboxamide synthase (E.C.6.3.2.6, SAICAR-kinosynthase), which form a duet in the de novo biosynthetic pathway to purine nucleotides.[14,15]

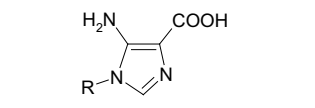

R = 1-β-D-ribofuranosyl 5'-phosphate

(**1**)

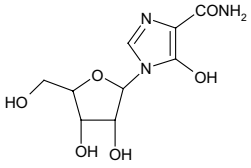

(**2**)

Keywords: Copper complexes; Amino-imidazole; Antimelanomal compounds; X-ray structure.

* Corresponding authors. Tel.: +1-614-2926336; fax: +1-614-2924118 (U.S.); tel.: +91-20-5696061; fax: +91-20-5691728/25693899 (S.P.); e-mail addresses: sandbhor.1@osu.edu; sbpadhye@chem.unipune.ernet.in

† Present address: Department of Molecular and Cellular Biochemistry, The Ohio State University, 433 Hamilton Hall, 1645 Neil Avenue, Columbus, OH 43210, USA.

0960-894X/$ - see front matter © 2004 Elsevier Ltd. All rights reserved.
doi:10.1016/j.bmcl.2004.03.041

Bredinin (**2**), is an imidazole derivative related to **1** and is isolated from the culture media of *Eupenicillium brefeldianum* M-2166. It is found to be a potent antibiotic against most microorganisms, except for *Candida albicans*[16–18] and has been of clinical use in Japan as an immuno-suppressant for the post-transplant patients.[19] This compound also possesses additional biological activities, which include antitumour,[18,20,21] antiviral,[16] antimalarial[22] and antiarthritic,[23,24] respectively. The core structural motif responsible for these broad spectrum biological activities is thought to be the imidazole aglycone, viz., 4-carbamoylimidazole-5-olate, which brings about competitive inhibition of purine nucleotides through the formation of a metal–substrate conjugate.[25] In our earlier communication we described the synergistic enhancement of antitumour activity of the imidazole ligand, 5-amino-1-tolylimidazole-4-carboxylate upon metal conjugation.[26]

In the present paper we describe the preparation and structural characterization of the copper(II) complexes of two 5-amino-imidazole-4-carboxylate derivatives and their antiproliferative activity against B16F10 mouse melanoma cells, which clearly shows the advantages gained by copper complexation of these ligands.

2. Experimental

All chemicals employed in the present work were purchased from Aldrich Chemicals (USA), and were used as received. All solvents used were of reagent grade and were purified by standard procedures prior to their use. The details of all experimental measurements and cell culture methods are as described earlier.[26,27]

3. Synthesis

Ligands were synthesized using a five-steps route as described previously.[28–31] Single crystals of L_1 and L_2, suitable for X-ray diffraction studies were grown by a slow evaporation of the respective ligand solutions in acetonitrile.

Copper complexes **MC1** and **MC2** were synthesized using an identical procedure (Scheme 1) as described below for the former compound.

Preparation of $[Cu(L_1)_2(H_2O)]\cdot 2H_2O$ (**MC1**) was carried out by doing an alkaline hydrolysis of the ligand $\mathbf{L_1}$,[26] yielding the corresponding acid, which was further reacted with the solution of $Cu(NO_3)_2\cdot 3H_2O$ in a metal: ligand ratio of 1:2 in methanol maintaining the pH of the reaction mixture at 7.0 by addition of 2 M sodium acetate. The reaction mixture was refluxed for 2 h and then stored in a refrigerator overnight to yield a green precipitate of **MC1**. The compound was recrystallized from methanol/water (9:1) solvent.

3.1. X-ray crystallography of L_1 and L_2

All measurements were made on a Siemens R3m/v diffractometer with Mo-Kα radiation (0.7107 Å). The data were collected at 293 K on a crystal of both ligands. Full matrix least squares refinement of the setting angles yielded a monoclinic cell. Based on the systematic absences, packing considerations, statistical analysis of the intensity distribution and the solution refinement of the structures and space groups were determined. The structures were solved by direct methods.[32,33] Full matrix least squares refinements gave weighted and unweighted agreement of residual factors.

Crystallographic data have been deposited with the Cambridge Crystallographic Data Centre, 12 Union Road, Cambridge, CB2 1EZ, UK (fax: +44-1223-336033; e-mail: deposit@ccdc.cam.ac.uk) and are available on request quoting the deposition number CCDC 205225 and 205226.

4. Results and discussions

4.1. Structural data and compositional studies

Single crystal X-ray structures of the ligands $\mathbf{L_1}$ and $\mathbf{L_2}$ were determined and their crystallographic parameters are listed in Table 1. The ORTEP diagrams together with the numbering schemes for these ligands are presented in Figures 1 and 2 along with their bond distances and bond angles.

Single crystal X-ray structures of both the ligands show that their geometries are highly distorted around the plane of the five-membered imidazole ring by the substitutions, viz. amino group at C(5)-position, carboxylate group at C(4)-position and the aromatic substitution at C(1)-position (Figs. 1 and 2). The substitution of $–CH_2–Ph$ group at N(1) position of the imidazole ring in $\mathbf{L_1}$ is held away from NH_2 group and is directed towards

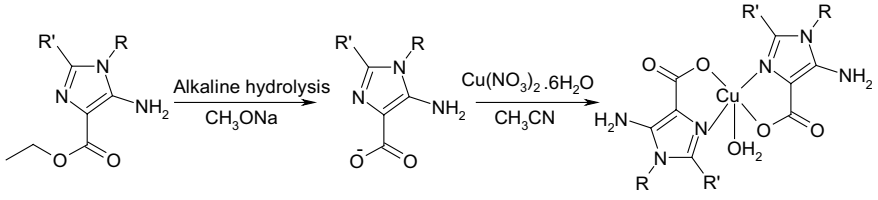

Scheme 1. Synthetic route for preparation of the copper complexes.

Table 1. Crystal data and structure refinement for ligands L_1 and L_2

	L_1	L_2
Empirical formula	$C_{13}H_{15}N_3O_2$	$C_{14}H_{17}N_3O_2$
Crystal size	$0.35 \times 0.20 \times 0.15\,mm^3$	$0.4 \times 0.25 \times 0.1\,mm^3$
Formula weight	245.28	259.31
Temperature	293 (2) K	293 (2) K
Wavelength	1.54178 Å	0.71073 Å
Crystal system	Monoclinic	Monoclinic
Space group	$P21/c$	$P21/c$
Unit cell dimensions	$a = 12.369(2)$ Å, $\alpha = 90°$	$a = 8.735(3)$ Å, $\alpha = 90°$
	$b = 8.2747(10)$ Å, $\beta = 92.94(2)°$	$b = 12.940(3)$ Å, $\beta = 95.92(4)°$
	$c = 12.279(4)$ Å, $\gamma = 90°$	$c = 12.010(5)$ Å, $\gamma = 90°$.
Volume	1255.1 (5) Å^3	1350.4 (8) Å^3
Z	4	4
Density (calculated)	1.298 Mg/m^3	1.275 Mg/m^3
Absorption coefficient	0.735 mm^{-1}	0.088 mm^{-1}
$F(000)$	520	552
Theta range for data collection	3.58°–65.24°	2.32°–25.01°
Index ranges	$-14 \leqslant h \leqslant 14$, $-9 \leqslant k \leqslant 9$, $-13 \leqslant l \leqslant 13$	$-10 \leqslant h \leqslant 9$, $0 \leqslant k \leqslant 15$, $-14 \leqslant l \leqslant 14$
Reflections collected	4164	4701
Independent reflections	2082 [$R_{(int)} = 0.1017$]	2372 [$R_{(int)} = 0.0592$]
Completeness to $\theta = 65.24°$	96.5%	99.6%
Refinement method	Full-matrix least-squares on F^2	Full-matrix least-squares on F^2
Data/restraints/parameters	2082/0/224	2372/0/240
Goodness-of-fit on F^2	1.048	0.974
Final R indices [$I > 2(I)$]	$R_1 = 0.0430$, $wR_2 = 0.0951$	$R_1 = 0.0463$, $wR_2 = 0.0893$
R indices (all data)	$R_1 = 0.0833$, $wR_2 = 0.1120$	$R_1 = 0.1126$, $wR_2 = 0.1110$
Largest diff. peak and hole	0.174 and −0.136 e Å^{-3}	0.163 and −0.206 e Å^{-3}

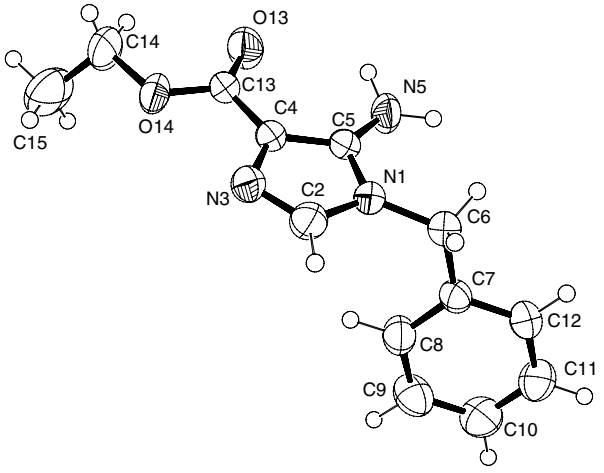

Figure 1. ORTEP diagram (in 50% ellipsoid level), bond lengths (Å) and bond angles (°) of ligand L_1. Bond lengths (Å), O(13)–C(13) 1.208 (3), O(14)–C(13) 1.336 (2), O(14)–C(14) 1.450 (4), N(1)–C(5) 1.364 (3), N(1)–C(2) 1.378 (3), N(1)–C(6) 1.454 (3), C(2)–N(3) 1.292 (3), N(3)–C(4) 1.393 (3), C(4)–C(5) 1.388 (3), C(4)–C(13) 1.435 (3), C(5)–N(5) 1.359 (3), C(6)–C(7) 1.511 (3), C(7)–C(12) 1.385 (3), C(7)–C(8) 1.385 (3), C(8)–C(9) 1.385 (3), C(9)–C(10) 1.372 (4), C(10)–C(11) 1.371 (4), C(11)–C(12) 1.374 (3), C(14)–C(15) 1.450 (5). Bond angles (°), C(13)–O(14)–C(14) 117.4 (2), C(5)–N(1)–C(2) 106.54 (17), C(5)–N(1)–C(6) 128.13 (18), C(2)–N(1)–C(6) 125.3 (2), N(3)–C(2)–N(1) 112.8 (2), C(2)–N(3)–C(4) 105.34 (17), C(5)–C(4)–N(3) 109.48 (19), C(5)–C(4)–C(13) 125.6 (2), N(3)–C(4)–C(13) 124.94 (17), N(5)–C(5)–N(1) 123.55 (18), N(5)–C(5)–C(4) 130.5 (2), N(1)–C(5)–C(4) 105.85 (18), N(1)–C(6)–C(7) 115.0 (2), C(12)–C(7)–C(8) 118.5 (2), C(12)–C(7)–C(6) 118.4 (2), C(8)–C(7)–C(6) 123.03 (18), C(9)–C(8)–C(7) 120.2 (2), C(10)–C(9)–C(8) 120.3 (3), C(11)–C(10)–C(9) 119.8 (2), C(10)–C(11)–C(12) 120.1 (2), C(11)–C(12)–C(7) 121.0 (2), O(13)–C(13)–O(14) 123.3 (2), O(13)–C(13)–C(4) 124.09 (18), O(14)–C(13)–C(4) 112.6 (2), C(15)–C(14)–O(14) 110.2 (3).

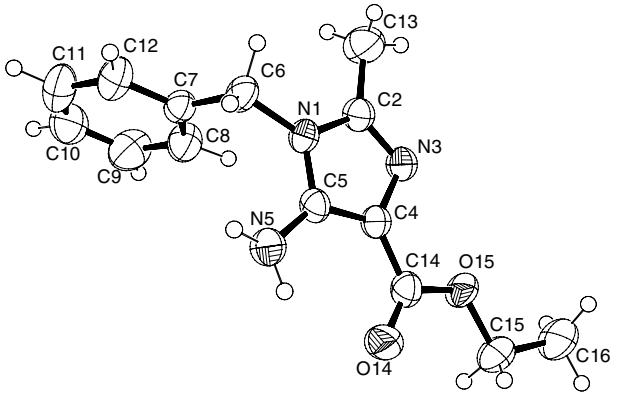

Figure 2. ORTEP diagram (in 50% ellipsoid level), bond lengths (Å) and bond angles (°) of ligand L_2. Bond lengths (Å), N(1)–C(5) 1.356 (3), N(1)–C(2) 1.381 (3), N(1)–C(6) 1.463 (3), C(2)–N(3) 1.301 (3), C(2)–C(13) 1.472 (4), N(3)–C(4) 1.383 (3), C(4)–C(5) 1.371 (3), C(4)–C(14) 1.425 (3), C(5)–N(5) 1.351 (3), C(6)–C(7) 1.495 (4), C(7)–C(8) 1.365 (3), C(7)–C(12) 1.384 (3), C(8)–C(9) 1.385 (4), C(9)–C(10) 1.371 (4), C(10)–C(11) 1.358 (4), C(11)–C(12) 1.372 (4), C(14)–O(14) 1.216 (3), C(14)–O(15) 1.343 (3), C(15)–O(15) 1.443 (3), C(15)–C(16) 1.485 (4). Bond angles (°), C(5)–N(1)–C(2) 106.58 (18), C(5)–N(1)–C(6) 126.1 (2), C(2)–N(1)–C(6) 127.2 (2), N(3)–C(2)–N(1) 111.7 (2), N(3)–C(2)–C(13) 125.7 (2), N(1)–C(2)–C(13) 122.6 (2), C(2)–N(3)–C(4) 105.6 (2), C(5)–C(4)–N(3) 109.7 (2), C(5)–C(4)–C(14) 125.3 (2), N(3)–C(4)–C(14) 125.0 (2), N(5)–C(5)–N(1) 122.6 (2), N(5)–C(5)–C(4) 130.9 (2), N(1)–C(5)–C(4) 106.4 (2), N(1)–C(6)–C(7) 114.6 (2), C(8)–C(7)–C(12) 118.1 (3), C(8)–C(7)–C(6) 123.3 (2), C(12)–C(7)–C(6) 118.5 (2), C(7)–C(8)–C(9) 120.6 (3), C(10)–C(9)–C(8) 120.2 (3), C(11)–C(10)–C(9) 119.8 (3), C(10)–C(11)–C(12) 120.0 (3), C(11)–C(12)–C(7) 121.3 (3), O(14)–C(14)–O(15) 122.5 (2), O(14)–C(14)–C(4) 124.3 (2), O(15)–C(14)–C(4) 113.3 (2), O(15)–C(15)–C(16) 107.2 (3), C(14)–O(15)–C(15) 117.6 (2).

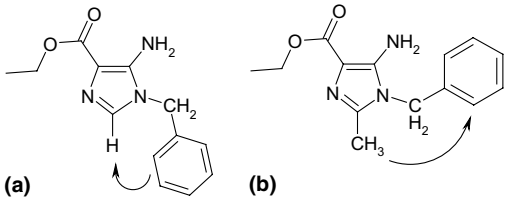

Scheme 2. Schematic representation shows repulsion of the phenyl ring towards amino group due to presence of extra methyl group at C(2) carbon.

C(2) carbon as shown in Scheme 2a while in the ligand **L_2** the methyl group at C(2) position is responsible for the displacement of aromatic ring towards amine nitrogen due to the steric repulsion as shown in Scheme 2b. The bond distances and bond angles differ slightly in **L_1** and **L_2** due perhaps to the electron donating methyl group around imidazole ring in ligand **L_2**.

The elemental analyses of complexes are listed in Table 2, which reveal 1:2 stoichiometries for the copper compounds accompanied by three water molecules, one of which is coordinated to the central copper atom. The formation of complexes can thus be represented by the following general equation: $2L + Cu(NO_3)_2{\cdot}2H_2O \rightarrow [Cu(L)_2(H_2O)]{\cdot}2H_2O$.

4.2. Spectroscopy and magnetism

The significant peaks in the IR spectra of copper compounds are listed in Table 2. The broad band at 3250–3460 cm^{-1} in the IR spectrum of the copper complexes is assigned to the coordinated water molecule.[26] The band at 3414 cm^{-1} in the spectra of ligands is assigned to NH_2 stretching vibration, which is found to remain unaffected even after metal complexation suggesting that it is not involved in coordination. On the other hand the vibrational frequencies due to the carboxylate and C=N of the imidazole linkages are shifted by 28–44 cm^{-1} upon metal complexation indicating their involvement in copper coordination.

The electronic spectra of copper complexes show a d–d absorption band in the range of 13,158–15,635 cm^{-1} (Table 3), which can be assigned to the $d_z^2 \rightarrow d_{x^2-y^2}$ transition.[34] This band appears in the usual range commonly observed for the square planar N_2O_2 donor groups and a weak axial coordination of the solvent oxygen.[35–37] For example, the square pyramidal copper complex, viz. $[Cu(2\text{-pic})(NO_3)_2]$, where pic = picolinic acid also shows absorption around 15,000 cm^{-1}.[38] In case of the complex **MC2**, the broad absorption band around 14,000 cm^{-1} is resolved into three bands at 15,635, 14,245 and 13,158 cm^{-1}, which are assigned to $d_z^2 \rightarrow d_{xz}/d_{yz}$, $d_z^2 \rightarrow d_{x^2-y^2}$ and $d_z^2 \rightarrow d_{xy}$ transitions, respectively. This is a typical spectral feature of the complexes with lower stereo symmetry[36] and is probably the result of solvent coordination at the vacant sixth site in solution. Examples of such solvent coordination have been noted in the case of coordinatively unsaturated copper complexes of bipyridine and acetylacetone (acac) ligands.[35,39] Additionally, present copper complexes exhibit a band of high intensity around 30,000–33,000 cm^{-1}, attributed to the ligand to metal charge transfer (LMCT) transition. Similar absorption has been observed in other analogous copper imidazole compounds.[40–43]

The X-band EPR spectra for the copper complexes were obtained in DMSO solvent and the calculated EPR parameters are listed in Table 3. The observed spin only magnetic values for the copper complexes suggest $S = 1/2$ spin ground state for these complexes[44,45] while the EPR spectral features are typical of compounds having D_4h symmetry with $g_\perp = 2.55$ and $g_\parallel = 3.05$, respectively. Slightly higher $A_\parallel$ values (163×10^{-4} cm^{-1}) are similar to those observed in the case of the mono-

Table 2. Compositional data and significant peaks in infrared spectra of copper complexes

Compound	Elemental analyses[a]				IR (cm^{-1})		
	%C	%H	%N	%Cu	ν(OH) coordinated	$\nu(COO^-)$	ν(CN)
MC1	48.78 (48.04)	4.28 (4.73)	15.42 (15.29)	11.90 (11.56)	3380	1642	1578
MC2	49.14 (49.87)	5.56 (5.19)	14.48 (14.54)	11.69 (11.00)	3368	1630	1575

[a] Values in parentheses are calculated values.

Table 3. Electronic spectral data, redox potentials, EPR and magnetic data of copper complexes

Compound	$\mu_{eff.}$ (BM)	$E_{1/2}$ (V)	EPR[a]			UV–vis[b] λ_{max} (cm^{-1})	Assignment
			$g_\perp$	$g_\parallel$	$A_\parallel$ (10^{-4}) cm^{-1}		
MC1	1.92	0.06	2.55	3.05	163	15,635	$d_z^2 \rightarrow d_{xz}/d_{yz}$
						14,245	$d_z^2 \rightarrow d_{x^2-y^2}$
						13,158	$d_z^2 \rightarrow d_{xy}$
						32,680	LMCT
MC2	1.89	0.10	2.55	3.04	153	14,493	$d_z^2 \rightarrow d_{x^2-y^2}$
						30,303	LMCT

[a] At 300 K.
[b] λ_{max} in DMSO solvent, LMCT; ligand to metal charge transfer band.

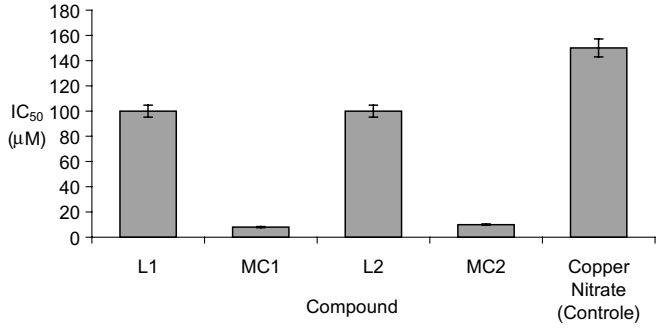

Figure 3. 50% Inhibition concentration (IC_{50}) values of ligands and their copper complexes against B16F10 mouse melanoma cells.

nuclear copper(II) complexes with square pyramidal geometries.[46–48]

The room temperature magnetic moments of the present copper complexes are determined using the Faraday method and are found to be around 1.90 BM (Table 3), which is typical for the copper complexes with square pyramidal geometries.[49] The values suggest no intermolecular interactions in the present case.

4.3. Cyclic voltammetry

The cyclic voltammograms of the copper complexes were recorded in DMSO solvent and the corresponding $E_{1/2}$ values are listed in Table 3. Copper compounds show a strong reduction peak in the range +0.06 to +0.10 V corresponding to the Cu(II)/Cu(I) redox couple.[50] An irreversible oxidation peak around −0.20 V corresponds to the oxidation of these ligands resulting in a partial dissociation of the complex. The positive potentials observed for the copper redox-couples in the present compounds suggest feasibility of their facile intracellular reduction.

4.4. Antimelanomal activity

Dose-dependent survival rates were obtained by treatment of the B16F10 melanoma cultures with the present copper complexes at physiological pH. The ligands and copper complexes are stable in biological environment. The IC_{50} values, which are calculated from dose–response curves, are from average of three repeated experiments, for the copper complexes range from 8–15 μM (Fig. 3). These values are substantially lower than those observed for the parent ligands (>50 μM) or the starting metal salt, viz. copper nitrate (>100 μM), respectively.

In conclusion, these results illustrate the advantage of copper conjugation in designing antimelanomal agents through its synergetic effect on the antiproliferative activity. The facile intracellular reduction of the copper ions in the present compounds (promoted by their positive redox potentials) and their subsequent interactions with cellular thiols has been postulated as the possible mechanism for the anticancer activity of such copper conjugates.[51]

Acknowledgements

U.S., P.K. and S.P. would like to thank the British Council for the visitorships under HE link programme. Thanks are also due to Ms. Sabari Dutta for the technical help.

References and notes

1. Cocco, M. T.; Congiu, C.; Plumitallo, A.; Schivo, M. L.; Palmieri, G. *Farmaco* **1987**, *42*, 347.
2. Cocco, M. T.; Congiu, C.; Maccinono, A.; Plumitallo, A.; Schivo, M. L.; De Logu, A. *Farmaco* **1989**, *44*, 975.
3. Cocco, M. T.; Olla, C.; Onnis, V.; Schivo, M. L.; De Logu, A. *Farmaco* **1992**, *47*, 229.
4. Varoli, L.; Burnelli, S.; Garuti, L.; Vitali, B. *Farmaco* **2001**, *56*, 885.
5. MacDonald, R. N.; Cairncross, A.; Sieja, J. B.; Aharkey, W. H. *J. Polym. Sci., Polym. Chem. Ed.* **1974**, *12*, 664.
6. Bouck, K. J.; Rasmussen, P. G. *Macromolecules* **1993**, *26*, 2077.
7. Rasmussen, P. G.; Kolowich, J. B.; Bayon, J. C. V. *J. Am. Chem. Soc.* **1988**, *110*, 7042.
8. Rasmussen, P. G.; Andresen, J. G.; Bayon, J. C. *Inorg. Chim. Acta* **1984**, *87*, 159.
9. Rasmussen, P. G.; Bayon, J. C. V. *Inorg. Chim. Acta* **1984**, *87*, 115.
10. Thurber, E. L.; Subrayan, R. P.; Rasmussen, P. G. *Contemporary topics in Polymer Science*; Plenum: New York, 1992; p 95.
11. Thurber, E. L.; Rasmussen, P. G. *J. Polym. Sci., Part A: Polym. Chem. Ed.* **1993**, *1*, 351.
12. Weber, G. *J. Med. Chem.* **1977**, *296*, 486.
13. Jackson, R. C.; Morris, H. P.; Weber, G. *Biochem.* **1977**, *166*, 1.
14. Mackenzie, G.; Shaw, G.; Thomas, S. E. *J. Chem. Soc., Chem. Commun.* **1976**, 453.
15. Mackenzie, G.; Shaw, G. *J. Chem. Res. (S)* **1977**, 184.
16. Mizuno, K.; Tsujino, M.; Takada, M.; Hayashi, M.; Atsmi, K.; Asuno, K.; Matsuda, T. *J. Antibiot.* **1974**, *27*, 775.
17. Yoshioka, H.; Nakatsu, K.; Hayashi, M.; Mizuno, K. *Tetrahedron Lett.* **1975**, *16*, 4031.
18. Sakaguchi, K.; Tsujino, M.; Yoshizawa, M.; Mizuno, K.; Hayano, K. *Cancer* **1975**, *35*, 1643.
19. Inou, T.; Kusaba, R.; Takahashi, I.; Sugimoto, H.; Kuzuhara, K.; Yamada, Y.; Yamauchi, J.; Otsubo, O. *Transplant. Proc.* **1981**, *8*, 315.
20. Sakaguchi, K.; Tsujino, M.; Hayashi, M.; Kawai, K.; Mizuno, K.; Hayano, K. *J. Antibiot.* **1976**, *29*, 1320.

21. Mizuno, K.; Mizayaki, T. *Chem. Pharm. Bull.* **1976**, *24*, 2248.
22. Webster, H. K.; Whaun, J. M. *J. Clin. Invest.* **1982**, *70*, 461.
23. Iwata, H.; Iwaki, H.; Mazukawa, T.; Kasamatsu, S.; Okamoto, H. *Experientia* **1976**, *33*, 502.
24. Koyama, H.; Tsuji, M. *Biochem. Pharm.* **1983**, *32*, 3547.
25. Shionoya, M.; Kimura, E.; Shiro, M. *J. Am. Chem. Soc.* **1993**, *115*, 6730.
26. Collins, M.; Ewing, D.; Mackenzie, G.; Sinn, E.; Sandbhor, U.; Padhye, S.; Padhye, S. *Inorg. Chem. Commun.* **2000**, *3*, 453.
27. Murugkar, A.; Padhye, S.; Guha-Roy, S.; Wagh, U. *Inorg. Chem. Commun.* **1999**, *2*, 545.
28. Conrad, M.; Shulze, A. *Chem. Ber.* **1909**, *42*, 743.
29. Mackenzie, G.; Wilson, H. A.; Shaw, G. In *Nucleic Acid Chemistry, Improved and New Synthetic Procedure, Methods and Techniques, PT 4*; Townsend, L. B., Tipson, R. S., Eds.; John Wiley & Sons, 1991; p 131.
30. Logemann, F. I.; Shaw, G. *Chem. Ind.* **1980**, 541.
31. Mackenzie, G.; Wilson, H. A.; Shaw, G.; Ewing, D. *J. Chem. Soc., Perkin Trans. 1* **1988**, 2541.
32. Sheldrick, G. M. SHELXTL-NT v.5.1; Bruker AXS: Madison, WI, USA, 1997.
33. Gilmore, C. *J. Appl. Crystallogr.* **1984**, *17*, 42.
34. Cameron, A. F.; Nuttall, R. H.; Taylor, D. W. *J. Chem. Soc., Chem. Commun.* **1970**, 865.
35. Hathaway, B. J. In *Comprehensive Coordination Chemistry*; Wilkinson, G., Gillard, R. D., McCleverty, J. A., Eds.; Pergamon: Oxford, 1987; Vol. 5, pp 594–774.
36. Lever, A. B. P. *Inorganic Electronic Spectroscopy*; 2nd ed.; Elsevier: Amsterdam, 1984.
37. Dung, N.-H.; Viossat, B.; Busnot, A.; Gotierrez, J. N.; Gardette, F. *Inorg. Chim. Acta* **1990**, *174*, 145.
38. Sutton, D. *Electronic Spectra of Transition Metal Complexes*; McGraw-Hill: London, 1968.
39. Bedford, R. L.; Clavin, M.; Belford, G. *J. Chem. Phys.* **1957**, *26*, 1165.
40. Pandiyan, T.; Palaniandavar, M.; Lakshminarayanan, M.; Manohar, H. *J. Chem. Soc., Dalton Trans.* **1992**, 3377.
41. Van Albada, G. A.; Lakin, M. T.; Veldman, N.; Spek, A. L.; Reedijk, J. *Inorg. Chem.* **1995**, *34*, 4910.
42. Van Albada, G. A.; Smitts, W. J. J.; Spek, A. L.; Reedijk, J. *Inorg. Chim. Acta* **1997**, *260*, 151.
43. Bernarducci, E.; Bharadwaj, P. K.; Krogh-Jespersen, K.; Potenza, J. A.; Schugar, H. J. *J. Am. Chem. Soc.* **1983**, *105*, 3860.
44. Fitzgerald, W.; Murphy, B.; Tyagi, S.; Walsh, B.; Walsh, A.; Hathaway, B. J. *J. Chem. Soc., Dalton Trans.* **1981**, 2271.
45. Price, J. M.; Pilbrow, J. R.; Murry, K. S. *J. Chem. Soc. (A)* **1970**, 968.
46. Bertini, I.; Gatteschi, D.; Scozzafava, A. *Inorg. Chem.* **1976**, *15*, 203.
47. Gerloch, M.; McMeeking, R. F. J. *J. Chem. Soc., Dalton Trans.* **1975**, 2443.
48. Da Silva, A. S.; Da Silva, M. A. A.; Carvalho, C. E. M.; Antunes, O. A. C.; Herrera, J. O. M.; Brinn, I. M.; Mangrich, A. S. *Inorg. Chim. Acta* **1999**, *292*, 1.
49. Morrison, B. *Acta Crystallogr.* **1969**, *25B*, 19.
50. Patterson, G. S.; Holm, R. H. *Bioinorg. Chem.* **1975**, *4*, 1975.
51. Reed, C. J.; Douglas, K. T. *Biochem. J.* **1991**, *275*, 601.